ORIGINAL PAPER

Sediment transport in furrow irrigation

**Damodhara R. Mailapalli · N. S. Raghuwanshi ·
R. Singh**

Abstract Irrigation-induced erosion in furrow irrigation causes loss of fertile soil and water quality degradation. Hence, quantification of irrigation-induced erosion is essential for efficient management of furrow irrigation. In this study, sediment transport was studied under bare and cropped field conditions for a furrow plot consisting of three parabolic shaped furrows of 40 m long and 0.5% slope. The inflow rates of 0.2, 0.3, 0.4 and 0.5 L s^{-1}; and 0.3, 0.4, 0.5, 0.6 and 0.7 L s^{-1} were used for bare and cropped field conditions, respectively. The furrow cross section measured at every 5 m distance from the head end (before and after the irrigation event) was used to study the erosion pattern (erosion/deposition) along the furrow. The runoff collected at regular intervals of 10 min was used to study the sediment load. The total sediment export for an irrigation event was estimated using furrow cross-section data (FCD) and the sediment rate data (SRD), and compared with the total sediments collected at the tail end. For both bare and cropped conditions, soil erosion took place at the head and tail ends (free drain system), while the deposition occurred at the middle. The sediment transport increased initially and slightly decreased with time. A power relationship was obtained between the total sediment export and the inflow rate for bare furrow condition, whereas a linear relationship between these parameters was obtained for cropped field

condition. The relative percentage errors suggested that both SRD and FCD methods can be used to estimate total sediment export from the field. The analysis (PSD) of the total sediments revealed that the geometric mean diameter of the sediment particle was 0.18 and 0.20 mm for bare and cropped field conditions, respectively.

Introduction

Furrow irrigation is one of the oldest and most widely used surface irrigation methods. The method generally has low capital investment and has potential for the efficient use of water and energy resources while maintaining high levels of crop production. However, this method may pose higher erosion and pollution risks than drip or even sprinkler irrigation methods. The effect of side slopes and concentrated water flow in the furrows may cause serious soil loss and disperse the agrochemicals adsorbed to the sediments into the environment (Agassi et al. 1995). Consequently, the desire to reduce the degradation of the surface water quality by sediments and agrochemicals has prompted new research on irrigation-induced erosion (Trout 1996; Bjorneberg et al. 1999; Strelkoff et al. 2002; Fernández Gómez et al. 2004) in furrow irrigation.

Erosion on irrigated land can have an adverse effect on soil fertility and, thus, on crop yield. Mech and Smith (1967) measured the soil losses of 67–134 t ha^{-1} from furrow-irrigated potato field. Carter et al. (1985) reported 25% decrease in the productivity of the soils in south-central Idaho due to irrigation-induced erosion over the preceding 80 years. They reported that the average wheat yield decreased to half as topsoil depths decreased from 38 to 13 cm, a yield decrease of 2% per cm of soil. A potential

D. R. Mailapalli (✉)
Department of Land, Air and Water Resources,
University of California, Davis, CA 95616, USA
e-mail: dam.iitkgp@gmail.com; dmailapalli@ucdavis.edu

N. S. Raghuwanshi · R. Singh
Agricultural and Food Engineering Department,
Indian Institute of Technology, Kharagpur 721302, India

yield decrease, without an equivalent decrease in expenses, is reflected in decreased potential profits for the farmers. Therefore, the erosion of yesterday costs the farmers today. Consequently, soil erosion will outlay more in future if corrective measures are not taken to control it. Hence, it is essential to quantify the irrigation-induced erosion for understanding the erosion mechanism in furrows, managing the irrigation system and minimizing environmental pollution.

Several studies have focused on quantification of erosion under various field and management conditions for the last two decades. Berg and Carter (1980) reported that furrow erosion varied considerably during an irrigation season. Generally, irrigations early in the season cause more erosion and sediment loss than later irrigations because initially the soil is dry and loose. Fornstrom and Borelli (1984) reported that soil loss for the first irrigation after cultivation was 60–100% greater than that for previously irrigated furrows. Mateos and Giráldez (2005) also reported that sediment load was greatest in the first irrigation and declined in successive irrigations. The furrow erosion assessments have usually been based on the measured sediment discharge from the outflow ends of the furrows or fields (Trout 1996). These discharge measurements are used to calculate the average soil loss per unit field area.

An accurate assessment of irrigation-induced erosion under different field conditions is essential for developing a proper management plan for erosion and pollution control. Therefore, the present research attempted to study the sediment transport and erosion pattern along the furrow, to quantify the total sediment export and to study the aggregate size of the sediments that are more prone to erosion in furrow irrigation.

Materials and methods

Experimental setup

Furrow irrigation experiments were conducted on a 4 m × 60 m plot in the Field Water Management Laboratory, Agricultural and Food Engineering Department, Indian Institute of Technology, Kharagpur, India. The physical properties of the field soil (sandy loam) are presented in Table 1. The experimental plot contained three 40 m-long, 0.30 m-wide and 0.15 m-deep freedrained furrows of parabolic shape. These furrows were spaced at 0.8 m and had a uniform slope of 0.5%. Among the three furrows, the center furrow was considered as the study furrow and the two side furrows served as the buffer to the center furrow. Figure 1 shows the schematic view of the experimental setup showing the center furrow.

Inlet setup

The inlet setup included water source (sump), inlet water tank and water delivery system. During the furrow experimentation, water from the sump was pumped to the inlet water tank and delivered to the furrows by the water delivery system (Fig. 1). The delivery system consisted of a 76.2 mm-diameter PVC pipe (main), to convey and distribute water from inlet tank to furrows through three PVC pipes of 50.8 mm diameter (sub main). Each sub main consisted of an inlet valve at the junction with the main pipe, digital flow meter, bypass and delivery valves. At the beginning of the experiment, the delivery and bypass valves were fully closed and opened, respectively, and allowed the flow through the bypass. The bypassed flow was measured manually using bucket and stopwatch by adjusting the inlet valve. The inlet valve was turned until the measured flow rate was equal to that desired. The flow rate was also cross-checked with the reading on the display unit of the digital flow meter (wheel type). The digital flow meters were installed based on the manufacturer's recommendations (keeping the sub main always with a full pipe flow) to minimize the effect of turbulent non-uniform flow at the inlet valve on the meter reading. The water was introduced to the furrow via a semi-circular PVC channel (0.15 m diameter and 0.3 m length) laid between the delivery point and the furrow. The PVC channel facilitates irrigation water to flow directly into the furrow and controls water spilling onto the soil surface (below the delivery), which helps in keeping the soil surface dry at the inlet

Table 1 Soil physical properties of the experimental plot

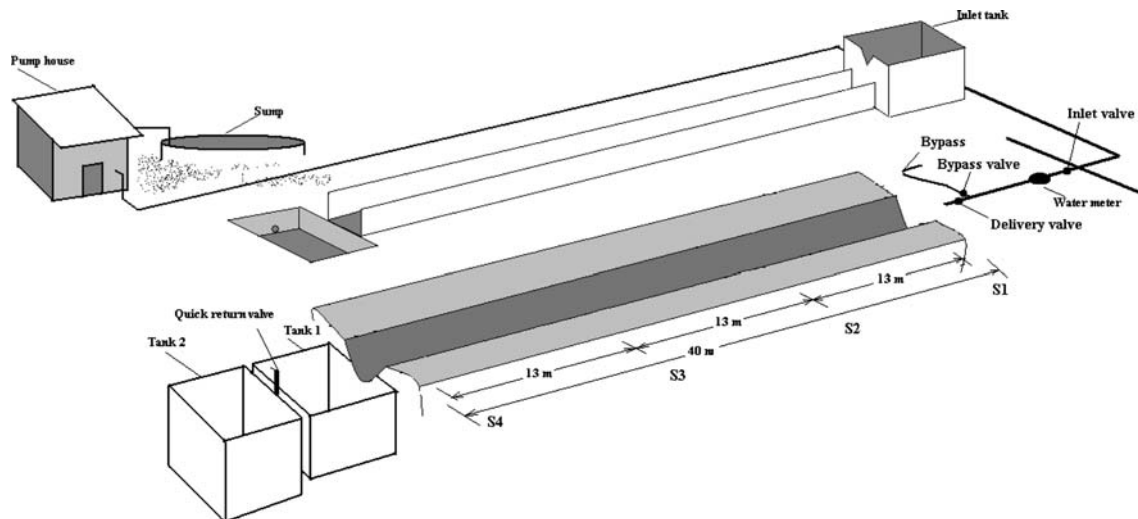| Depth (m)	Sand (%) (2–0.05 mm)	Silt (%) (0.05–0.002 mm)	Clay (%) (<0.002 mm)	Porosity (%)	Particle density (g cm^{-3})	Bulk density (g cm^{-3})	Organic matter (%)
0–0.15	69	17	14	40	2.56	1.54	0.43
0.15–0.30	66	19	15	39	2.54	1.56	0.32
0.30–0.45	63	21	16	38	2.55	1.58	0.26
0.45–0.60	60	24	16	38	2.58	1.61	0.17

451

Fig. 1 Schematic view of the experimental setup showing the center furrow

during the irrigation experiment. The irrigation water to the three furrows was started at the same time by closing the bypass valve and opening the delivery valve simultaneously.

Outlet setup

The outlet setup consisted of two rectangular tanks (Fig. 1) made of acrylic sheet (size: 1 m × 1 m × 1 m) and buried at the tail end, with the first tank placed 0.15 m above the second tank to facilitate free drainage of water to the second tank through a horizontal pipe connecter at the bottom. A quick return valve was fitted at the center of the horizontal pipe (between tanks 1 and 2) to cut the flow to the second tank while measuring the water level. The quick return valve opens and closes the horizontal pipe quickly to facilitate flow from tank 1 to 2. When the water level of tank 1 attained three-fourths of its capacity, the quick return valve was closed to cut off the flow to tank 2. At this instant, the water from tank 2 was drained and the quick return valve was opened for filling tank 2 again. Water samples were collected at 10-min time intervals from the tail end of the center furrow (study furrow) using a plastic container of 3 L capacity, and the time taken to fill each container was noted for measuring the runoff rate.

Experimentation

The irrigation experiments were conducted on 6, 17, 21 and 29 February 2004 using constant inflow rates of 0.2, 0.3, 0.4 and 0.5 L s^{-1}, respectively, on bare furrow field. In 2005, the field was cropped with sunflower (*Helianthus annuus* L.) in four rows having plant-to-plant and row-to-

row spacing of 0.45 and 0.80 m, respectively. The sowing was done on 27 February 2005. The experiments were conducted on 3 and 30 March, 9 April, and 16 and 23 May 2005 with constant inflow rates of 0.7, 0.6, 0.5, 0.4 and 0.3 L s^{-1}, respectively. The constant inflow rate was set before each irrigation event with digital flow meters and control valves as described in the previous section. Table 2 shows the summary of the irrigation experiments performed under bare and cropped field conditions during the years 2004 and 2005, respectively.

Data and methodology

The data including furrow cross section, runoff (rate and volume), sediment load and export were used to quantify and study the sediment transport. Before and after an irrigation event, profilometer was used to measure the furrow cross section at 0.5, 5, 10, 15, 20, 25, 30, 35 and 39.5 m distance from the head end of the study furrow. These nine locations are referred, hereafter, as $L_1, L_2, L_3, L_4, L_5, L_6, L_7, L_8$ and L_9, respectively. The cross-section data of a location contained 15 rod lengths (profilometer) representing the depths from the bed to the perimeter of the section (Mailapalli et al. 2008). The three (0.02 m spaced) middle rod lengths were used to estimate the average furrow depth of a location. The difference in furrow depths of the locations obtained before and after the irrigation was used to study the sediment transport (erosion or deposition) along the furrow and to quantify the sediment export from the furrow. Figure 2 shows the conceptualization of the furrow cross section change along a segment after an irrigation event. The amount of soil eroded or deposited for a furrow segment was estimated by assuming the shape change as trapezoidal. The

Table 2 Summary of the furrow experiments conducted during the years 2004 and 2005

Field condition	Date	Inflow (L s^{-1})	Irrigation time (min)	Advance (min)	Recession (min)	Obs. inflow (m^3)	Outflow (m^3)	Infiltration (m^3)
Bare	6 Febuary 2004	0.2	145	27.50	2.50	1.76	0.65	1.11
	17 Febuary 2004	0.3	120	12.28	2.70	2.17	0.74	1.43
	21 Febuary 2004	0.4	120	08.58	2.90	2.87	1.13	1.56
	29 Febuary 2004	0.5	130	05.66	2.80	4.00	2.40	1.60
Cropped	3 March 2005	0.7	60	4.76	3.05	2.54	1.70	0.84
	30 March 2005	0.6	60	5.40	2.70	2.14	1.21	0.93
	9 April 2005	0.5	60	6.40	2.50	1.80	1.02	0.78
	16 May 2005	0.4	60	10.20	3.25	1.46	0.74	0.72
	23 May 2005	0.3	60	11.63	3.26	1.07	0.37	0.70
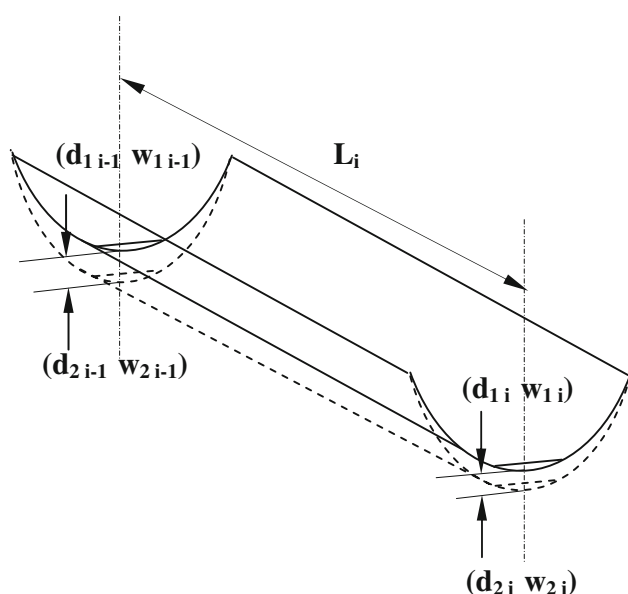
Fig. 2 Furrow cross section change of the segment

trapezoidal volume of soil eroded or deposited during an irrigation event was determined for each segment of length L and its mass was calculated by multiplying bulk density of the top 0.2 m of soil layer. The total sediment export from the furrow was determined by the sum of eroded or deposited soil mass of all segments using the following equation. The average change in cross section over the length of the furrow segment was assumed as the average of the product of the average change in width and the change in depth. This method of estimating sediment export is denoted by FCD.

$$E_{sed} = \frac{\rho}{4}\sum_{i=1}^{n} L_i\big[(d_{2,i-1} - d_{1,i-1}) \times (w_{2,i-1} + w_{1,i-1}) + (d_{2,i} - d_{1,i}) \times (w_{2,i} + w_{1,i})\big] \quad (1)$$

where E_{sed} is the sediment export, ρ is the bulk density of the topsoil, L is the length of the furrow segment, d_1 and d_2 are the average furrow depths before and after an irrigation event, w_1 and w_2 are the furrow bottom widths before and after an irrigation event and i is the index of furrow section.

At the end of the experiment, the water samples collected at the tail end at regular time intervals were labeled and taken to the laboratory for measuring the sediment load. The water samples were filtered through Whatman filter paper# 10 for 3–4 h. The mass of the sediment retained on each filter paper was determined using the oven dry method. The sediment load (g L^{-1}) was determined by dividing the mass in grams with the corresponding sample volume in liters. The rate of sediment flow (g s^{-1}) during the time interval was determined by multiplying the sediment load (g L^{-1}) with the corresponding runoff rate (L s^{-1}). The sediment export from the furrow was quantified by the sum of the product of the rate of the sediment flow and the corresponding time interval, and the method is denoted by SRD. At the end of irrigation, the sediments collected in the outlet tanks were oven dried and weighed to estimate the total sediment export, which was considered as reference sediment export (labeled as 'outlet tank') because it represents the actual sediment loss from the furrow (sediments lost through sampling were neglected). The proposed two methods for sediment export (i.e., FCD and SRD) were compared with the total sediments in the 'outlet tank'. Particle size distribution (PSD) analysis was carried out to determine particle sizes that were prone to irrigation-induced erosion and their geometric mean using the sediments collected in the tanks for each irrigation event.

Results and discussion

Erosion pattern along the furrow

Table 3 presents the average furrow depths along the furrow during the irrigations of 2004 and 2005 under bare and cropped field conditions, respectively. In case of a bare field, the furrow depth increased at locations L_2, L_3, L_4 and L_9 and decreased at L_1, L_6, and L_7 for the experiments conducted on 6 and 17 February 2004. At locations L_5 and L_8, the furrow depth did not change much and, therefore, these locations are considered to be under the transition phase. Transition phase is the time when the erosion phase changes to deposition phase and vice versa. For the irrigation experiments conducted on 21 and 29 February 2004, the furrow depth increased at L_2, L_3, L_4, L_5 and L_9 locations, whereas it decreased at L_1 and L_7 locations. The cross section remained same at locations L_6 and L_8. The transition point of irrigation events of 6th and 17th February (L_5) shifted to L_6 for irrigation events of 21 and 29 February 2004, which indicated that the transition phase shifts toward the tail end with increased flow rate. For cropped field, the furrow depth decreased at locations L_1, L_6 and L_7, which indicates the deposition of the soil (Table 3). At locations L_2, L_3, L_4 and L_9, the furrow depth, however, increased, which indicates the soil erosion at these locations. At locations L_5 and L_8, mild change in furrow depth was observed. Hence, these points are considered as the transition points.

The results revealed that for both bare and cropped fields, soil erosion in the furrows takes place at the head and tail ends (free drained furrows), while soil deposition occurs in the middle of the furrow. The water introduced into the furrow via PVC channel at the furrow head initially, picks up the soil particles and carries them down the furrow. At some point (i.e., locations L_6 and L_7 on both

bare and cropped conditions) along the furrow, the capacity of the flow to transport the accumulated sediment decreases and net deposition occurs (Trout 2001). Most of the sediment eroded at the head end of the field (i.e., L_2, L_3 and L_4) settles out before reaching the end of the furrow (i.e., L_9). Since the furrows are free drained, furrow stream velocity increases and again becomes erosive at the tail end.

Sediment transport

The variation of sediment load for irrigation events of 6, 17, 21 and 29 February 2004 with the elapsed time are shown in Fig. 3. The start and end points of the sediment graph depend on the time to cease advance and recession phases, respectively. The sediment load initially increased and thereafter slightly decreased with the elapsed time during each irrigation event. As described above, the water introduced into the furrow via PVC channel picks up the loose soil particles and carries them down the furrow. Furthermore, the loose soil particles may also create more
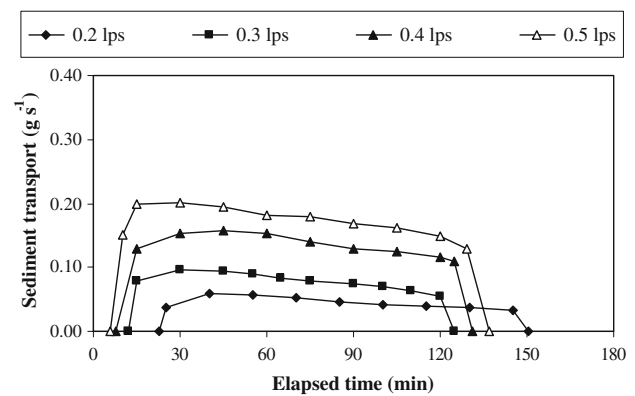

Fig. 3 Temporal variation of sediment load for the bare field condition

Table 3 Variation of furrow depth along the furrow during the years 2004 and 2005

Field condition	Irrigation date	Depth of furrow (cm) at various locations								
		L_1	L_2	L_3	L_4	L_5	L_6	L_7	L_8	L_9
Bare	Initial cross section	16.80	16.15	14.10	15.10	14.10	14.50	15.20	14.80	15.40
	6 Febuary 2004	16.75	16.55	14.35	15.35	14.20	14.10	15.00	14.60	15.95
	17 Febuary 2004	16.20	17.15	15.05	15.60	14.20	13.55	14.60	14.50	16.45
	21 Febuary 2004	15.60	17.54	15.85	15.74	14.25	13.54	14.30	14.55	16.65
	29 Febuary 2004	15.10	18.10	16.25	16.40	14.35	13.54	13.85	14.54	17.20
Cropped	Initial cross section	14.85	15.10	15.50	15.60	15.00	14.95	14.70	14.90	15.80
	3 March 2005	14.43	15.50	16.23	16.00	15.10	14.80	14.60	15.10	15.55
	30 March 2005	14.23	15.62	16.32	16.24	15.22	14.84	14.62	15.32	16.50
	9 April 2005	14.00	15.72	16.50	17.13	15.25	14.60	14.53	15.35	17.93
	16 May 2005	13.87	16.02	16.90	17.46	15.31	14.32	14.43	15.39	17.93
	23 May 2005	13.54	17.13	18.33	17.90	15.39	14.31	15.43	15.45	17.60

shears on the furrow bed to detach the soil particles. The combination of these two phenomena leads the initial increase of the sediment load. Later, the furrow stream continues to pick up sediment until its energy equals the energy needed to carry the soil particles. The furrow stream size and velocity decrease as it advances down the furrow. As the furrow stream's energy decreases, so does its ability to carry soil. This decrease in sediment load with time has been reported earlier (Brown et al. 1988; Trout and Neibling 1993; Trout 1996). Possible explanations for the sediment load trend include the initial flushing of loose aggregates created by rapid wetting, the stabilization of the furrow perimeter soil, and soil layer becoming more resistant to erosion. A similar trend in sediment loads was observed for all the irrigations. The sediment load increased with the inflow rate due to increased stream size and velocity. The initial increasing sediment loads in the subsequent irrigations were due to the inflow as well as the removal of the vegetation from the furrow (to make bare field), which likely weaken the bonds between the soil particles and result in more soil loss. The sediment export for an irrigation event was related to the corresponding inflow. The sediment export increased with the inflow and followed a power relationship (Fig. 4).

Figure 5 shows the variation of sediment load with the elapsed time for the irrigation events of 3 March, 30 March, 9 April, 16 May and 3 June 2005. The sediment load decreased with time, as was the case under the bare field condition. However, the amount of sediment discharged at the tail end was more than in the bare field condition. For example, the total amount of sediment collected from cropped field after 60 min time was found to be 0.40, 0.77 and 0.98 kg for 0.3, 0.4 and 0.5 L s^{-1} inflow rates compared to 0.30, 0.50 and 0.65 kg for the bare field condition. This may be due to drier profile and loosening of top layer due to inter-tillage operations in the cropped field. As in the case of bare field, the sediment yield for an irrigation event increased with the inflow and followed a linear relationship (Fig. 6). The linear relationship for cropped condition may be due to the shorter irrigation durations (60 min) than the bare furrow condition (120 min).

Estimation of sediment yield using SRD and FCD methods

In most of the cases, SRD estimated sediment yield close to the outlet tank than the FCD method for both bare and cropped field conditions (Figs. 7, 8). The performance of these methods was further studied by estimating the relative percentage errors. The average relative percentage error for SRD and FCD were within 10%, which is considered to be an acceptable range for most of the research studies. Therefore, both SRD and FCD methods proposed
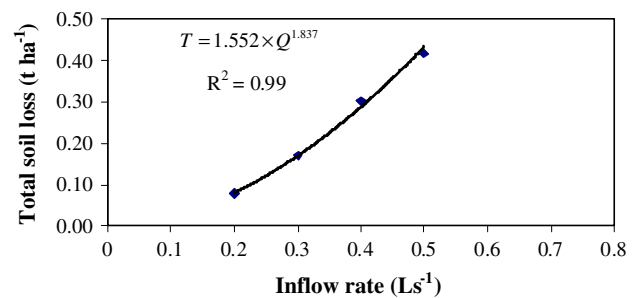
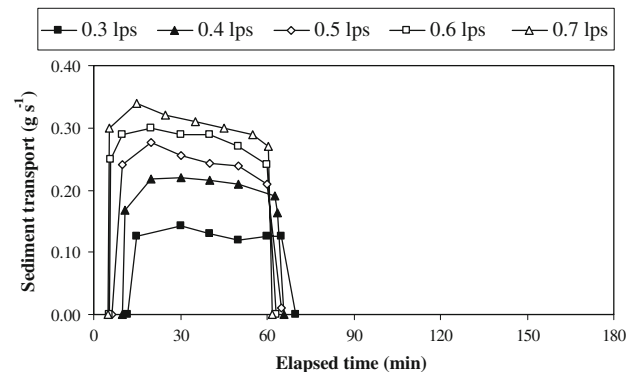**Fig. 4** Variation of total sediment load with inflow rate for the year 2004

Fig. 5 Variation of sediment load with elapsed time for the irrigations in 2005
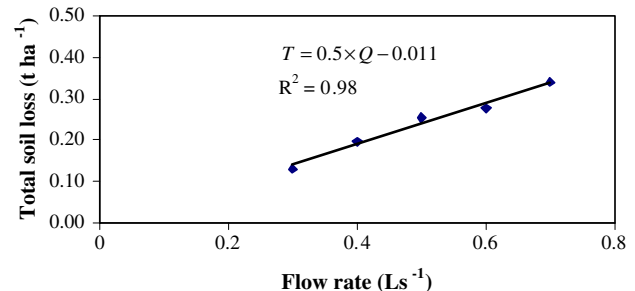

Fig. 6 Variation of total sediment load with inflow rate for the year 2005

in this study can be used to estimate average sediment yield in furrow irrigation.

Particle size distribution analysis

Table 4 presents the PSD analysis for the sediments collected during the irrigations of bare field. No particular trend was observed between the inflow rate and the percentage weight. Moreover, the weight of the particles having sizes in the range of 0.5–0.25, 0.25–0.125 and 0.125–0.053 mm is distributed equally. The geometric mean size of the particle was estimated as 0.18 mm for the bare field condition. Table 5 shows the PSD analysis of the
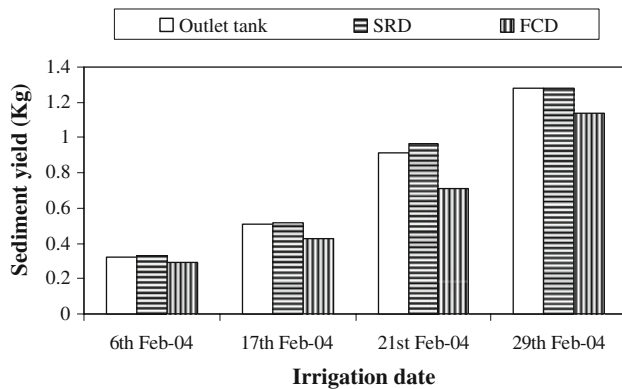
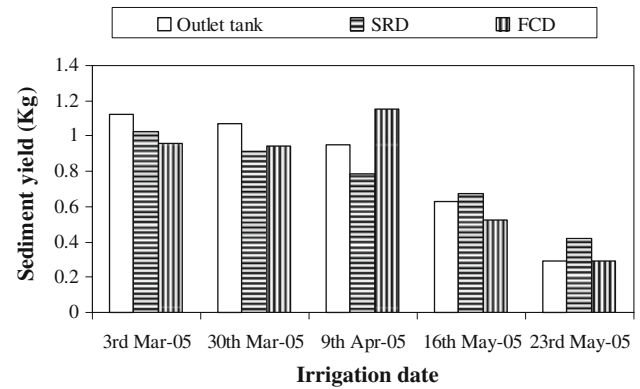**Fig. 7** Comparison of sediment yields estimated using various methods for 2004

Fig. 8 Comparison of sediment yields estimated using various methods for 2005

Table 4 PSD analysis of the sediment load for bare field condition

Sieving size (mm)	0.2 L s^{-1}		0.3 L s^{-1}		0.4 L s^{-1}		0.5 L s^{-1}	
	Percentage weight	Percent finer	Percentage weight	Percent finer	Percentage weight	Percent finer	Percentage weight	Percent finer
>1	2.10	100.00	3.30	100.00	3.70	100.00	2.80	100.00
1–0.5	11.30	86.60	13.20	83.50	14.20	82.10	13.40	83.80
0.5–0.25	24.10	62.50	25.40	58.10	24.60	57.50	25.40	58.40
0.25–0.125	23.40	39.10	23.80	34.30	21.50	36.00	21.30	37.10
0.125–0.053	24.60	14.50	20.30	14.00	19.40	16.60	23.50	13.60
0.053–0.035	6.50	8.00	4.50	9.50	6.40	10.20	5.30	8.30
<0.035	8.00	0.00	9.50	0.00	10.20	0.00	8.30	0.00

Table 5 PSD analysis of the sediment load for cropped field condition

Sieving size (mm)	0.7 L s^{-1}		0.6 L s^{-1}		0.5 L s^{-1}		0.4 L s^{-1}		0.3 L s^{-1}	
	Percentage weight	Percent finer	Percentage weight	Percent finer	Percentage weight	Percent finer	Percentage weight	Percent finer	Percentage weight	Percent finer
>1	3.40	100.00	3.10	100.00	2.70	100.00	2.20	100.00	2.40	100.00
1–0.5	15.60	81.00	12.40	84.50	12.60	84.70	14.50	83.30	13.10	84.50
0.5–0.25	25.20	55.80	26.50	58.00	27.30	57.40	26.30	57.00	24.70	59.80
0.25–0.125	18.50	37.30	20.30	37.70	20.40	37.00	17.30	39.70	22.30	37.50
0.125–0.053	19.80	17.50	19.90	17.80	18.50	18.50	23.50	16.20	22.60	14.90
0.053–0.035	7.30	10.20	6.50	11.30	8.40	10.10	4.80	11.40	5.50	9.40
<0.035	10.20	0.00	11.30	0.00	10.10	0.00	11.40	0.00	9.40	0.00

total sediments collected at the end of the irrigation event on cropped field. As in the case of the bare field, no particular trend was observed between the inflow rate and the percentage weight for cropped field. However, for some size ranges, the percentage weight retained decreased with the decreased inflow rate. The weight of the particles having sizes ranging from 0.5 to 0.25 mm is more prone to erosion under cropped field condition. The geometric mean size of the soil particles was estimated as 0.2 mm.

Conclusions

In this study, the erosion pattern along the furrow, the sediment load trends, estimation of sediment load using FCD and SRD, and the PSD analysis of the eroded soil collected from the tail end were studied for bare and cropped furrow field. The soil erosion took place at the head and tail ends (free drained), while the deposition occurred in the middle of the furrow for both bare and

cropped fields. This indicates that the runoff from a furrow field contains bed load from the tail end. Since the sediment of the upstream is deposited in the middle of furrow, the tail end sediment into the runoff can be controlled by installing partial dams (earthen/plastic) at the tail end. This may result in good quality of runoff to the downstream water or soil bodies. The study also suggested that the sediment yield methods (FCD and SRD) gave acceptable results. Using the particle size analysis of the sediments, the geometric mean diameter of the particles was found to be 0.18 and 0.20 mm for bare and cropped furrow conditions, respectively. The information on the size of sediment being transported by water in the furrow is useful for verifying erosion simulation results. Predicting sediment size distributions is important because smaller aggregates tend to carry more nutrients per unit mass than larger ones (enrichment ratio).

References

Agassi M, Letey J, Farmer WJ, Clark P (1995) Soil erosion contribution to pesticide transport by furrow irrigation. J Environ Qual 24:892–895

Berg ED, Carter DL (1980) Furrow erosion and sediment losses in irrigated cropland. J Soil Water Conserv 35:367–370

Bjorneberg DL, Trout TJ, Sojka RE, Aase JK (1999) Evaluating WEPP-predicted infiltration, runoff, and soil erosion for furrow irrigation. Trans ASAE 42:1733–1742

Brown MJ, Kemper WD, Trout TJ, Humpherys AS (1988) Sediment erosion and water intake in furrows. Irrig Sci 9:45–55

Carter DL, Berg RD, Sanders BJ (1985) The effect of furrow irrigation erosion on crop productivity. Soil Sci Soc Am J 49:207–211

Fernández Gómez R, Mateos L, Giráldez JV (2004) Furrow irrigation erosion and management. Irrig Sci 23:123–131

Fornstrom KJ, Borelli J (1984) Design and management procedure for minimizing erosion from furrow-irrigated cropland. Paper No. 84-2595. ASAE, St. Joseph, MI

Mailapalli DR, Raghuwanshi NS, Singh R, Schmitz GH, Lennartz F (2008) Spatial and temporal variation of Manning's roughness coefficient in irrigation furrows. J Irrig Drain Eng 134(2):185–192

Mateos L, Giráldez JV (2005) Suspended load and bed load in irrigation furrows. Catena 64:232–246

Mech SJ, Smith DD (1967) Water erosion under irrigation. In: Hagan RM, Haise HR, Edminster TW (eds) Irrigation of agricultural lands. Agronomy monograph 11. ASA, Madison

Strelkoff TS, Fernández Gómez R, Mateos L, Giráldez JV, Clemmens AJ (2002) On tracking sediment particle sizes in furrow irrigation induced erosion for modeling phosphorus transport. In: Conference on energy, climate, environment and water: issues and opportunities for irrigation and drainage. July 9–12, 2002, San Luis Obispo, California

Trout TJ (1996) Furrow irrigation erosion and sedimentation: on-field distribution. Trans ASAE 39(5):1717–1723

Trout TJ (2001) Sediment transport in irrigation furrows. In: Stott DE, Mohtar RH, Steinhardt GC (eds) Sustaining the global farm: selected papers from the 1999 International Soil Conservation Organization meeting. W. Lafayette, IN, 24–29 May, 1999, pp 710–716

Trout TJ, Neibling WH (1993) Erosion and sedimentation process on irrigated fields. J Irrig Drain Eng 119(6):947–963